数例，長期予後を観察するために，医師主導治験を考えています．医師主導治験を申請しても時間がかかりますので，その前に高度医療を申請するということで，いま最終吟味に入っているという段階です．ほかには角膜内皮や実質の研究も行っています（Table 3）．

Table 3 標準治療へ向けた改良点

①安全性の向上にむけた改良
②バリデーション法の開発
③多数例，長期予後 高度医療，治験

＜Q&A＞

座長（永井） ありがとうございました．この治療法については，いろいろなプロセスがあって，3T3の問題，あるいはFBSの問題を一つずつ解決されつつあるということでした．先生，薬事の問題について，一言だけコメントいただけますか．高度医療にしても，いずれにせよ解決しないといけない問題ですね．

西田 そうですね．いまPMDA，厚生労働省と話をしているところで，ここで断言できるような状態にはありません．

Fig. 24 自家皮膚線維芽細胞フィーダーを用いた自家培養上皮細胞シートの作成

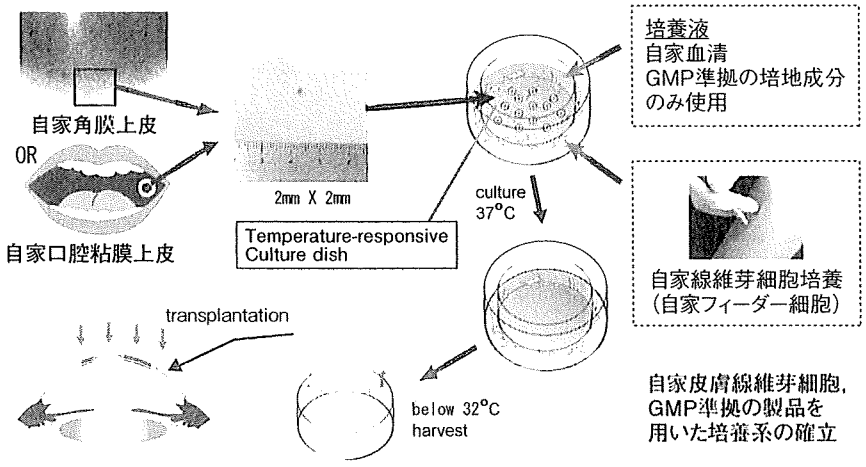

*　　*　　*

Histological evaluation of mechanical epithelial separation in epithelial laser in situ keratomileusis

Takeshi Soma, MD, Kohji Nishida, MD, PhD, Masayuki Yamato, PhD, Seiichi Kosaka, Joseph Yang, Ryuhei Hayashi, MSc, Hiroaki Sugiyama, MSc, Naoyuki Maeda, MD, PhD, Teruo Okano, PhD, Yasuo Tano, MD, PhD

PURPOSE: To evaluate the effect of mechanical epithelial separation with an epikeratome on the histologic ultrastructure of epithelial flaps and stromal beds from human corneas.

SETTING: Departments of Ophthalmology, Osaka University Medical School, Osaka, and Tohoku University School of Medicine, Sendai, and Institute of Advanced Biomedical Engineering and Science and Medical Research Institute, Tokyo Women's Medical University, Tokyo, Japan.

METHODS: Eye-bank eyes were deepithelialized using an Epi-K epikeratome. Epithelial flaps and stromal beds were assessed by light and electron microscopy. Immunofluorescence staining for types IV and VII collagens, integrins α_6 and β_4, and laminin 5 was also performed.

RESULTS: Four eyes were evaluated. On scanning electron microscopy, the cleavage planes of epithelial flaps and stromal beds were relatively smooth. On transmission electron microscopy, epithelial flaps were separated partially within the lamina fibroreticularis and partially within the lamina lucida. Immunofluorescence showed positive staining for type VII collagen and discontinuous staining for type IV collagen in stromal beds. Discontinuous linear staining for types IV and VII collagens was observed in epithelial flaps. Staining for integrins α_6 and β_4 was positive in some regions and discontinuous in other regions of epithelial flaps. In stromal beds, integrins α_6 and β_4 had a patchy expression pattern. Staining for laminin 5 was intermittently positive along the basal side of epithelial flaps and stromal beds.

CONCLUSIONS: Epithelial flaps created with an epikeratome were mechanically separated partly within the lamina fibroreticularis and partly within the lamina lucida. Stromal beds had relatively smooth surfaces with no obvious trauma to Bowman layer.

J Cataract Refract Surg 2009; 35:1251–1259 © 2009 ASCRS and ESCRS

Laser in situ keratomileusis (LASIK) is currently the most popular technique to surgically correct refractive errors. Compared with photorefractive keratectomy (PRK), LASIK provides several advantages including rapid visual recovery, reduced postoperative pain, and minimal corneal haze.[1,2] However, LASIK complications related to the corneal flap, such as buttonholes, free flaps, flap striae, epithelial ingrowth, and corneal ectasia, can develop postoperatively.[3–5]

In 1999, Camellin introduced laser-assisted subepithelial keratectomy (LASEK), a modification of conventional PRK. With this technique, an epithelial flap is created using a dilute ethanol solution to loosen the epithelial layer (U. Cimberle, "LASEK May Offer the Advantages of Both LASIK and PRK," Ocular Surgery News, March 1, 1999, page 28). After ablation, the epithelial flap is repositioned on the stromal bed. Therefore, LASEK can avoid the flap-related complications observed with LASIK because no stromal flap is created. Researchers report that LASEK is more effective than conventional PRK in the correction of moderate myopia[6,7] and that LASEK is better than LASIK in the uniformity of the corneal topography, corrected visual acuity, and contrast sensitivity 6 months postoperatively.[8] Despite these promising results, there are substantial concerns about the possible toxicity of ethanol to the epithelial flap and the underlying stroma after LASEK.[9,10]

In 2003, Pallikaris et al.[11] introduced the refractive surgical technique of epithelial LASIK (epi-LASIK). In this technique, an epithelial flap is created by mechanical separation using an epikeratome, a device

Published by Elsevier Inc.

doi:10.1016/j.jcrs.2009.02.025

similar to a microkeratome. After mechanical separation and photoablation on the underlying stromal bed, the epithelial flap is replaced on the stroma, similar to the LASEK method. Because epi-LASIK procedures do not require alcohol or other chemical agents to create an epithelial flap, researchers have theorized that mechanical separation can avoid the toxic effects of alcohol on the epithelial flap and stromal bed and provide an automated surgical procedure with a short learning curve for LASIK surgeons.[12]

During mechanical separation in epi-LASIK procedures, the points of anchoring between the corneal epithelium and stroma are cleaved. At these positions, hemidesmosomes normally connect the basal epithelial cells to the basement membrane. Within the hemidesmosomes of basal corneal epithelial cells, the transmembrane proteins integrin α_6 and integrin β_4 adhere to laminin 5, which is a major basement membrane component.[13,14] The basement membrane comprises 3 layers: the lamina lucida, the lamina densa, and the lamina fibroreticularis. The lamina densa is a sheet-like structure made up of the extracellular matrix (ECM) molecules type IV collagen, laminin, entactin–nidogen, and perlecan. The lamina fibroreticularis lies beneath the lamina densa, contains anchoring fibrils comprising type VII collagen, and forms a complex network with type I and type V collagens to attach the epithelium and its basement membrane to the underlying Bowman layer (Figure 1).[15–17]

Although the clinical outcomes of epi-LASIK have been evaluated,[18–20] the exact site of epithelial separation during epi-LASIK remains unclear. Pallikaris et al.[12] found that the epithelial separation was

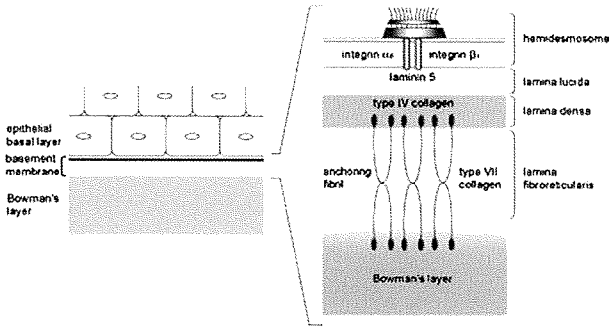

Figure 1. Schematic diagram of epithelial anchorage to the stroma. (Distances and sizes are not to scale.)

beneath the basement membrane with intact basal cells. Kollias et al.[21] found that the basal cell layer of the epithelial flap had normal morphology with interruptions of the basement membrane. However, Tanioka et al.[22] report that the basement membrane was lost and the basal cells were damaged in some regions. In addition, a detailed study of the cleavage planes in the epithelial flap and stromal bed in epi-LASIK has not been performed.

In the current study, we evaluated the cleavage plane of the epithelial flap mechanically separated with an epikeratome and the underlying stromal bed in epi-LASIK. We also identified details of the exact site of cleavage in the epithelial flap after mechanical separation.

MATERIALS AND METHODS

This study adhered to the tenets of Declaration of Helsinki regarding the use of human tissue specimens.

Mechanical Separation

Intact human donor eyes (Northwest Lions Eye Bank) were obtained 5 hours 16 minutes to 5 hours 28 minutes after donor death and stored in a conventional moist chamber for 3 to 6 days at 4°C. Epithelial separation was performed using the Epi-K epikeratome (Moria). This device has a disposable oscillating head (oscillation rate 15000 rpm) encasing a preassembled noncutting stainless-steel blade to mechanically separate the epithelial layer from the underlying stroma using 3 speeds (low, 0.05 mm/s; medium, 0.25 mm/sec; normal, 0.50 mm/s). The assembled head, handpiece, and suction ring were placed on the eye, and suction was activated. After adequate suction ($\geq$65 mm Hg) was confirmed by Barraquer tonometry and a stable reading of lower pressure on the epikeratome console was obtained, the oscillating head was advanced to the horizontal corneal plane at low speed. When the epithelial flap rose and was visible between the separator and the applanation plate, the device was shifted to medium speed, cleaving the epithelial layer. Just after the edge of the separator reached the center of the suction ring, the epithelial flap was cleaved at top speed. When the head reached the stopping point, the footpedal was released and low vacuum was activated. After a stable

Submitted: October 17, 2008.
Final revision submitted: February 13, 2009.
Accepted: February 19, 2009.

From the Departments of Ophthalmology, Osaka University Medical School (Soma, Sugiyama, Maeda, Tano), Osaka, and Tohoku University School of Medicine (Nishida, Hayashi), Sendai, and the Institute of Advanced Biomedical Engineering and Science (Yamato, Yang, Okano) and Medical Research Institute (Kosaka), Tokyo Women's Medical University, Tokyo, Japan.

No author has a financial or proprietary interest in any material or method mentioned.

Supported in part by the High-Tech Research Center Program and the Center of Excellence Program for the 21st Century from the Ministry of Education, Culture, Sports, Science, and Technology, Japan.

Corresponding author: Kohji Nishida, MD, PhD, Department of Ophthalmology, Tohoku University School of Medicine, 1-1 Seiryo-machi, Aoba-ku, Sendai, 980-8574, Japan. E-mail: knishida@oph.med.tohoku.ac.jp.

low-vacuum level was confirmed, the head was moved backward and the device was removed from the eye.

Tissue Processing

Immediately after epithelial separation, the epithelial flaps were excised along the hinge and trisected. The stromal beds were also excised from the globe and trisected. One of each of the specimens was placed in neutral buffered formalin 10% (Nacalai Tesque) and routinely processed for conventional histologic examination. Another specimen from each tissue was immersed in glutaraldehyde 2.0% (Nacalai Tesque) in 0.1 M phosphate buffer (pH 7.4) for scanning electron microscopy (SEM) and transmission electron microscopy (TEM). The third group of specimens was frozen in OTC compound (Tissue-Tec, Sakura Finite) for processing into frozen sections and subsequent immunofluorescence staining.

Histological Analysis

Formalin-fixed specimens were dehydrated with a graded series of ethanol, washed with xylene solution, and processed into 3 μm thick paraffin-embedded sections. Conventional hematoxylin–eosin staining was then performed, and the sections were visualized by light microscopy (BX50, Olympus).

Scanning Electron Microscopy

Glutaraldehyde-fixed specimens were rinsed in phosphate buffer and postfixed in osmium tetroxide 2% for 2 hours at 4°C. The specimens were then dehydrated through a graded series of ethanol and 3-methylbutyl acetate before critical-point drying. The samples were mounted on aluminum stubs, coated with an osmium plasma coater, and examined by SEM (S-4300, Hitachi High-Tech). Cleavage surfaces of the epithelial flaps and stromal beds were examined at 4 magnifications (×20, ×50, ×1000, ×10000).

Transmission Electron Microscopy

Glutaraldehyde-fixed specimens were rinsed in phosphate buffer and postfixed in osmium tetroxide 2% for 2 hours at 4°C. The specimens were dehydrated through a graded series of ethanol and methyl glycidyl ether and embedded in epoxy resin according to standard techniques. Semi-thin sections (5 μm) were then stained with toluidine blue, and a suitable area was chosen. The blocks were trimmed and thin-sectioned (100 nm), stained with uranyl acetate-Reynold lead nitrate 4%, and examined by TEM (H-7100 or H-7650, Hitachi High-Tech).

Immunofluorescence

Frozen specimens were cut into 10 μm-thick sections using a cryostat (Jung CM3000, Leica) at −20°C, mounted on glass slides coated with magnesium aluminosilicate glass, air dried, and stored at −80°C. Sections were incubated with a 1:20 dilution of polyclonal goat anticollagen IV (1340-01, Southern Biotechnology Associates), a 1:1000 dilution of monoclonal mouse anticollagen VII (LH 7.2, Sigma), a 1:100 dilution of monoclonal mouse antiintegrin α_6 (4F10, Chemicon International), a 1:200 dilution of monoclonal mouse antiintegrin β_4 (ASC-8, Chemicon International), or a 1:200 dilution of monoclonal mouse antilaminin 5 (P3H9-2, R&D Systems) overnight at 4°C. The sections were then incubated with fluorescein isothiocyanate-conjugated mouse anti-goat immunoglobulin G (IgG) or goat anti-mouse IgG (both Jackson ImmunoResearch Laboratories) for 2 hours at room temperature. The stained sections were counterstained with Hoechst 33342 for 10 minutes at room temperature to visualize the cell nuclei. Sections incubated identically with equal concentrations of normal mouse and goat Ig or a secondary antibody alone served as negative controls. All sections were viewed by confocal laser scanning microscopy (Fluoview FV1000, Olympus).

RESULTS

Four eye-bank eyes were used in the study.

Epithelial Flaps

Light microscopic examination of the epithelial flap showed that normal stratification and cell morphology were well preserved in all 4 eyes after mechanical separation using the epikeratome. No obvious trauma or blebs were observed in the basal cells of the epithelial flap (Figure 2).

Scanning electron microscopy of the epithelial flaps at low magnification (×50) showed that the bottom surface of the epithelial flap had a relatively smooth surface with little debris (Figure 3, *A*). At a magnification of ×1000, the underside of the epithelial flaps had regions of 2 differing thicknesses in all eyes (Figure 3, *B*). In the thinner regions, the basement membrane appeared to be mostly absent from the epithelial flap (Figure 3, *B*). In contrast, in the thicker regions, the basement membrane seemed to be present on the posterior surface of the epithelial flap (Figure 3, *B*). Overall, in all eyes the thin regions were mainly in the center of the epithelial sheets, resembling spot-like formations, while the thick regions were in the surrounding areas. At higher magnification (×10000), columnar structures and several depressions were seen in the areas of the epithelial flaps without a basement membrane (Figure 3, *C*). However, in the thick regions, the posterior surface of the basement membrane was relatively rough with numerous protuberances

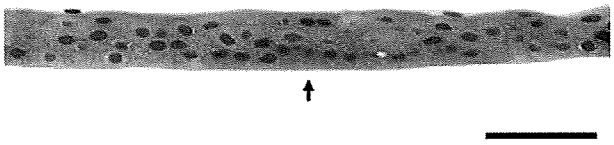

Figure 2. Light micrograph of an epithelial flap after mechanical separation. The arrow indicates the basal side of the epithelial sheet (*bar* = 50 μm).

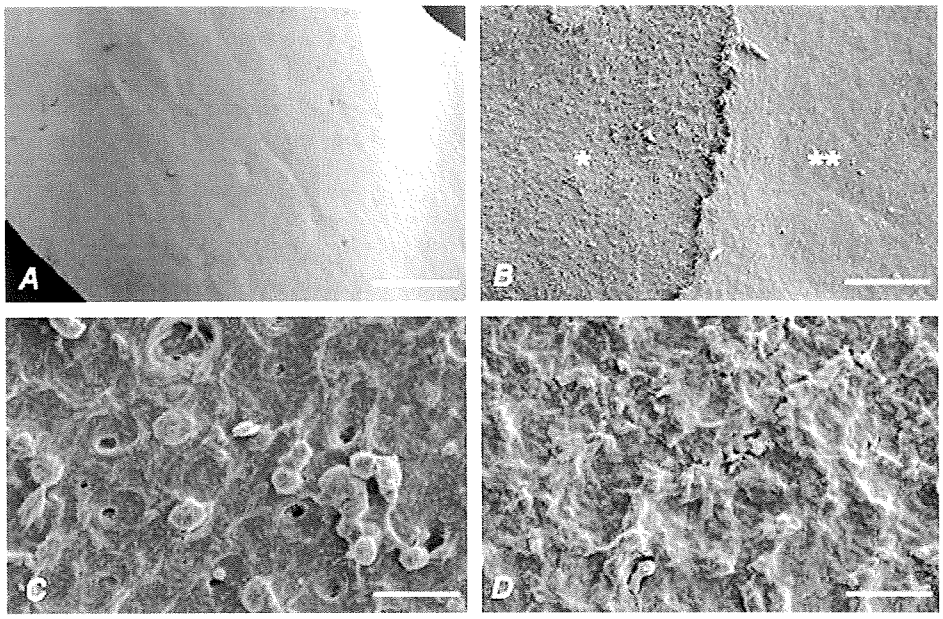

Figure 3. *A*: Scanning electron microscopy of an epithelial flap after mechanical separation at low magnification (×50) (*bar* = 200 μm). *B*: Higher magnification (×1000) view of the panel *A* shows a flap with no basement membrane in the thin regions (*single asterisk*) and a basement membrane on the basal side of the flap in the thick regions (*double asterisk*) (*bar* = 20 μm). *C*: High magnification (×10000) of the thin region of panel *B* shows columnar structures and some depressions on the posterior surface of the epithelial flap (*bar* = 2 μm). *D*: Higher magnification (×10000) of the thick region in panel *B* shows several crest-like protuberances on the underside of the epithelial flap (*bar* = 2 μm).

(Figure 3, *D*). No obviously disrupted basal cells were seen in any cleavage plane in the 4 eyes.

Transmission electron microscopy showed that the epithelial flaps had 2 cleavage planes in all eyes. The first plane was along the lamina lucida (Figure 4, *A*), and the second plane was within the lamina fibroreticularis (Figure 4, *B*). In regions of the epithelial flap where there was no basement membrane, the basal epithelial cells had fewer hemidesmosomes and several small blebs were observed (Figure 4, *A*). In these areas, the plasma membrane on the basal side of the epithelial cells was also occasionally disrupted. Light microscopy and SEM showed no obvious disruption of the basal cells. Hemidesmosome attachments were also cleaved with the lamina lucida.

In contrast, in other regions the epithelial flap was cleaved along with the entire lamina lucida, the intact lamina densa, and a portion of lamina fibroreticularis (Figure 4, *B*). Transmission electron microscopy showed that the basal epithelial cells and their intracellular contacts had normal morphology and that the anchoring of the hemidesmosomes to the basement membrane remained intact. In these regions, the epithelial flap was separated from the underlying stromal bed along with a portion of the basement membrane into the lamina fibroreticularis.

Immunostaining results showed discontinuous linear staining of type IV collagen along the basal side of the epithelial flaps (Figure 5, *A*). Staining for type VII collagen was consistent with that of type IV collagen at all sites (Figure 5, *B*). Integrin α_6 had 2 distinct patterns in the epithelial flaps after mechanical separation. Continuous linear expression of integrin α_6 was seen beneath the basal epithelial cells in some regions,

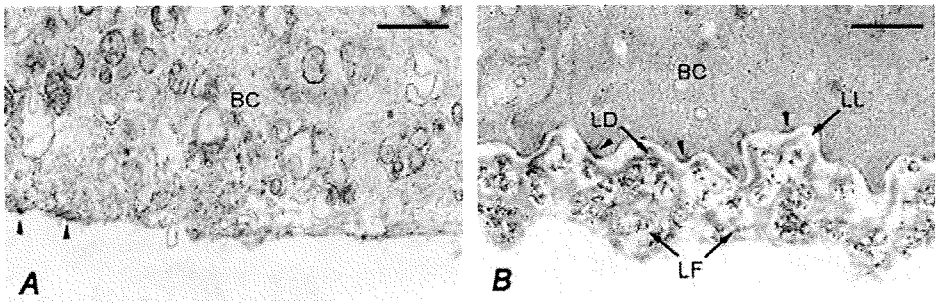

Figure 4. Transmission electron micrographs of epithelial flaps after mechanical separation. *A*: The epithelial flaps have no epithelial basement membrane. There are fewer hemidesmosomes (*arrowhead*) on the basal side of the epithelial basal cells (BC), which has several small intracellular blebs. *B*: The epithelial flap with the lamina lucida (LL), the lamina densa (LD), and part of the lamina fibroreticularis (LF). The cell morphology and intracellular structure of the basal cells (BC) are well preserved, and the hemidesmosomes (*arrowhead*) adhere to the basal lamina (*bars* = 200 nm).

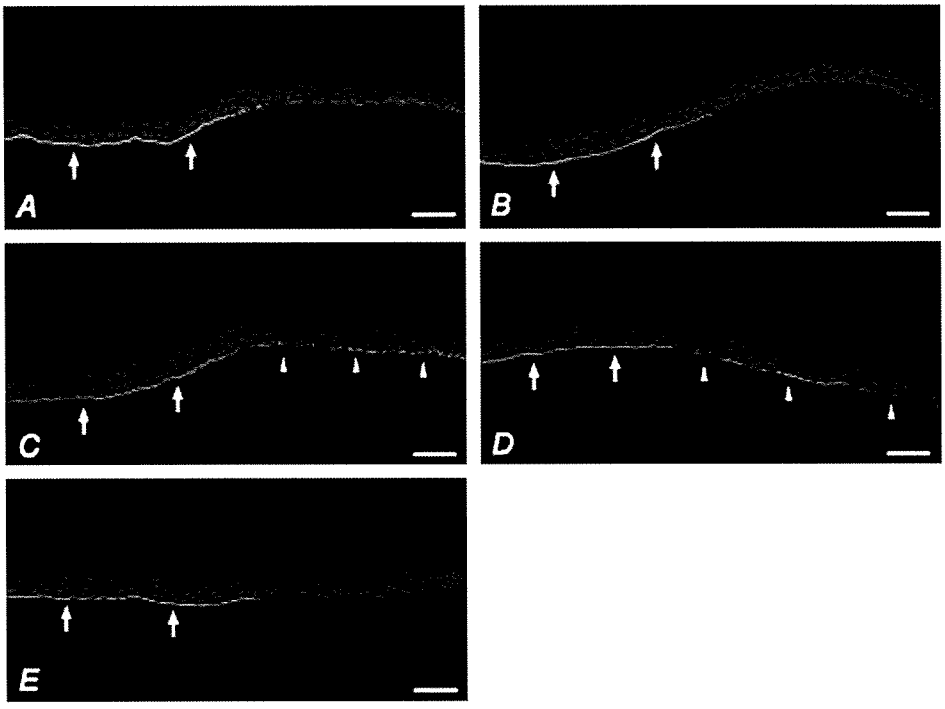

Figure 5. Immunostaining of an epithelial flap for types IV and VII collagens, integrin α_6 and β_4, and laminin 5. *A*: Discontinuous positive staining of type IV collagen along the basal side of the epithelial basal cells (*arrows*). *B*: Discontinuous positive staining of type VII collagen along the basal side of the epithelial basal cells (*arrows*). *C*: Linear staining (*arrows*) and patchy expression (*arrowheads*) of integrin α_6 along the bottom of the epithelial flap. *D*: Linear staining (*arrows*) and patchy expression (*arrowheads*) of integrin β_4 along the bottom of the epithelial flap. *E*: Discontinuous positive staining of laminin 5 along the basal side of the epithelial basal cells (*arrows*) (*bars* = 50 μm).

and inconsistent staining was observed in other areas (Figure 5, *C*). The staining patterns for integrin β_4 also had the 2 characteristic arrangements that were similar to those of integrin α_6 (Figure 5, *D*). Within the epithelial flaps, laminin 5 was expressed linearly along the basal side of the epithelial layers (Figure 5, *E*). These findings suggest that the cleavage plane of the epithelial flap was created within the lamina fibroreticularis in the regions of the positive staining for types IV and VII collagens, integrins α_6 and β_4, and laminin 5. In contrast, when epithelial separation was within the lamina lucida, no positive staining for types IV and VII collagens or laminin 5 was observed. The patchy staining of integrin α_6 and integrin β_4 suggests that epithelial flaps were not cleaved in the deeper regions of the lamina lucida but were cleaved only beneath the cell membrane of the basal cells.

Stromal Beds

Hematoxylin-eosin staining of the stromal beds showed that Bowman layer and the corneal stroma were well conserved after mechanical separation. All specimens also had smooth surfaces with no trauma to Bowman layer (Figure 6).

Scanning electron microscopy of the stromal beds at low magnification (×50) showed that the surface of the stromal beds was relatively smooth with little debris (Figure 7, *A*). High-resolution observation (×1000) of the surface of the stromal bed indicated that the exposed areas were mostly within Bowman layer; however, portions of the basement membrane were present in some regions (Figure 7, *B*). The 2 differing stromal surfaces were observed in all eyes. The regions of the stromal bed with portions of the basement membrane were generally seen as several island-like formations mainly in the center of the stromal bed, with the surrounding areas having mostly exposed regions of Bowman layer. At higher magnification (×10000), the anterior surface of the mostly exposed Bowman layer comprised a network of straight and curved fibers with some debris, which may have been part of the lamina fibroreticularis (Figure 7, *C*). In the regions with portions of the basement membrane, there were granular and amorphous components of the ECM on the surface of the basal lamina (Figure 7, *D*). At the

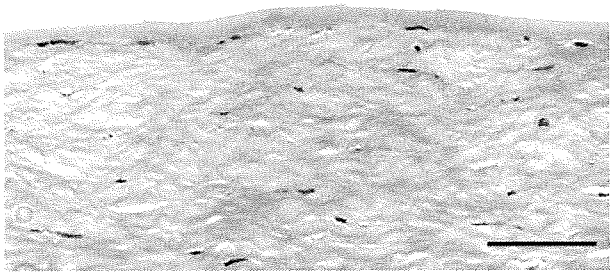

Figure 6. Light micrograph of a stromal bed after mechanical separation (*bar* = 50 μm).

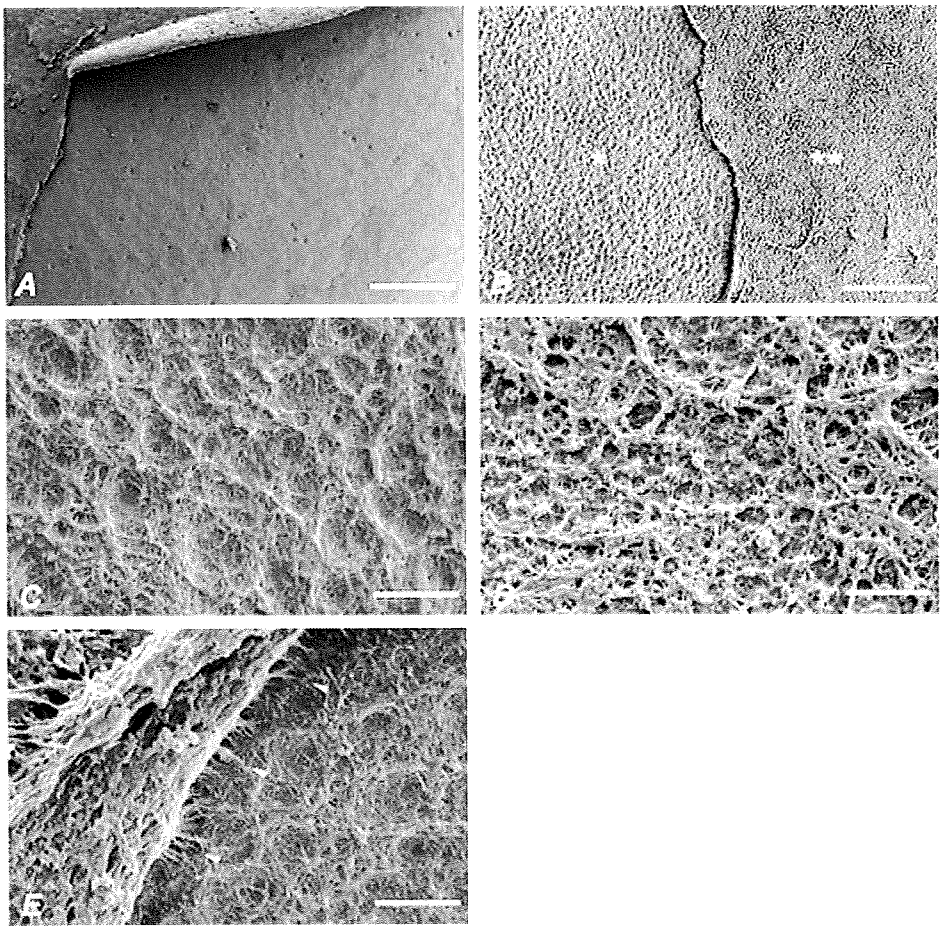

Figure 7. *A*: Scanning electron micrograph of a stromal bed after mechanical separation at low magnification (×50) (*bar* = 200 μm). *B*: Magnified view (×1000) of panel *A* (*bar* = 20 μm) shows partially exposed Bowman layer (*single asterisk*) and preserved basement membrane on the surface of the stromal bed in some areas (*double asterisk*). *C*: High magnification (×10 000) of the exposed Bowman layer (*bar* = 2 μm). *D*: High magnification (×10 000) of the remaining basement membrane on the stromal bed (*bar* = 2 μm). *E*: Magnified view (×10 000) of the interface between the basement membrane and Bowman layer shows numerous fibers adhering to both regions (*arrowheads*) (*bar* = 2 μm).

interface between the regions of the lamina densa and Bowman layer, numerous fibrils, likely the lamina fibroreticularis, adhered to both regions (Figure 7, *E*). No cleavage planes within Bowman layer or the corneal stroma were observed in the 4 eyes.

Transmission electron microscopy of the stromal beds showed 2 distinct cleavage planes, 1 at the level of the lamina fibroreticularis and the other at the level of the lamina lucida. In the former, portions of the lamina fibroreticularis that were approximately 100 to 200 nm thick were present above Bowman layer, indicating that mechanical separation occurred within the lamina fibroreticularis (Figure 8, *A*). In the latter, bundles of anchoring fibrils and the lamina densa were retained on Bowman layer (Figure 8, *B*), which showed that the epithelial flap was separated along the lamina lucida in these regions. For both cleavage planes, Bowman layer and the stroma had normal morphology with no trauma in either region.

When immunostaining for type IV collagen was performed, positive expression was observed only along the surface of Bowman layer (Figure 9, *A*). In contrast, there was positive staining for type VII collagen in all regions of the stromal surface (Figure 9, *B*). In the stromal beds, expression of integrin α_6 was discontinuous in some areas while other regions had no staining (Figure 9, *C*). Similarly, integrin β_4 showed patchy expression only in some regions of the stromal bed surfaces (Figure 9, *D*). Laminin 5 had discontinuous linear expression along the surface of Bowman layer (Figure 5, *E*). These results indicate that the epithelial flap was cleaved along the lamina lucida where types IV and VII collagens and laminin 5 were expressed and patchy patterns of integrin α_6 and β_4 were observed. These findings suggest that epithelial separation occurred within the upper regions of the lamina lucida. It also appears that the plane of cleavage during the epi-LASIK procedure was within the lamina fibroreticularis, which was negative for type IV collagen, integrin α_6 and β_4, and laminin 5 but positive for type VII collagen.

DISCUSSION

The current study identified 3 major histological characteristics of the epithelial flaps and stromal beds

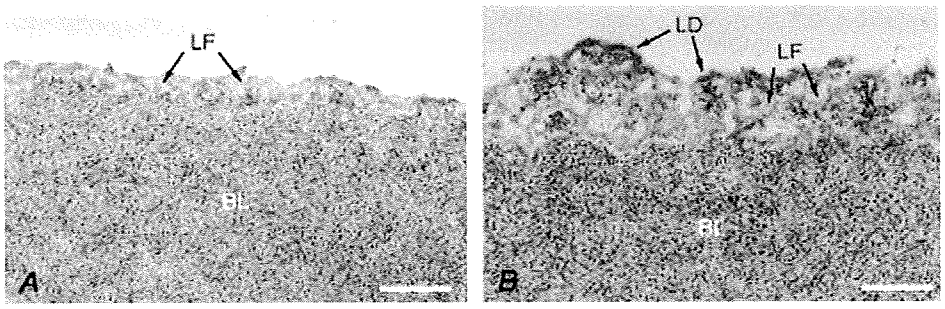

Figure 8. Transmission electron micrographs of stromal beds after mechanical separation. *A*: The lamina fibroreticularis (LF) comprised of anchoring fibrils is preserved at a thickness of 100 to 200 nm on Bowman layer (BL). *B*: The lamina densa (LD) and lamina fibroreticularis (LF) are present on Bowman layer (BL) (*bars* = 200 nm).

created during epi-LASIK using an epikeratome. First, Bowman layer and the underlying corneal stroma remained intact after epithelial separation. Second, the cleavage planes of the epithelial flap and the stromal beds were relatively smooth. Finally, the epithelial flap was mechanically separated at 2 cleavage planes in some regions along the lamina lucida and in the lamina fibroreticularis in other regions.

In the current study, we report what we believe is the first histologic evaluation of the characteristics of the corneal stromal bed after mechanical separation using the Epi-K epikeratome. There was no obvious trauma to Bowman layer or the underlying stroma in the stromal beds after mechanical separation, suggesting that epi-LASIK performed using this epikeratome is safe and avoids complications (eg, microstriae,

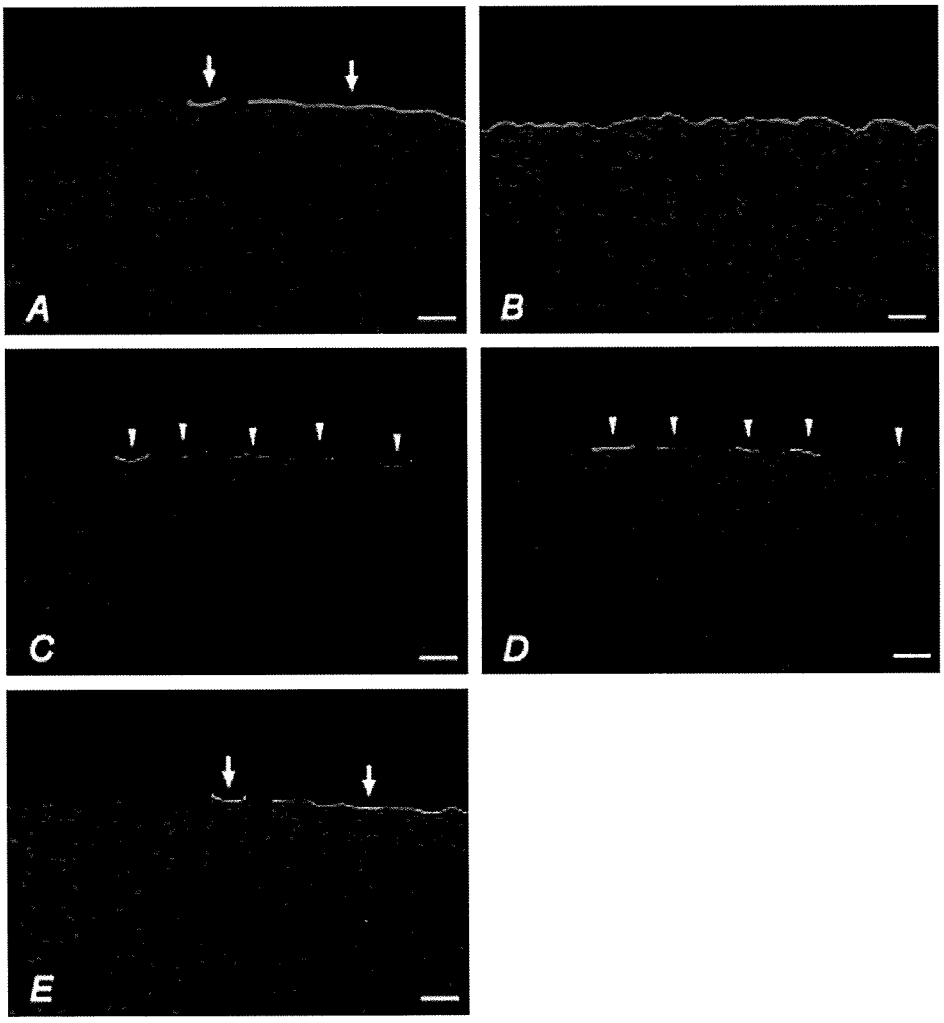

Figure 9. Immunostaining of a stromal bed for types IV and VII collagens, integrin α_6 and β_4, and laminin 5. *A*: Discontinuous positive staining for type IV collagen along the surface of the stromal bed (*arrows*). *B*: Positive staining for type VII collagen in all regions of the stromal bed. *C*: Patchy staining of integrin α_6 along the stromal surface (*arrowheads*). *D*: Patchy staining of integrin β_4 along the stromal surface (*arrowheads*). *E*: Discontinuous positive staining of laminin 5 shows along the surface of the stromal bed (*arrows*) (*bars* = 100 μm).

epithelial ingrowth) that can occur at the stromal interface after LASIK.[3]

We also found that most of the stromal surfaces contained regions with Bowman layer mostly exposed in approximately two thirds of the entire stromal bed area and that portions of the basement membrane, with thickness ranging from 100 to 200 nm, remained on the stromal surface in the other area. These results indicate that mechanical separation with the epikeratome we used provides a relatively smooth underlying bed surface before photoablation. A smooth stromal bed theoretically reduces postoperative corneal haze and irregular astigmatism, which can lead to less predictable visual results.[23] Moreover, compared with LASEK, epi-LASIK may create a similarly smooth stromal surface without use of topical alcohol, which can be toxic to the epithelial flap and stromal bed.

The epikeratome we used separates the epithelial layer from the underlying stroma using 3 speeds. The device is shifted from low speed to medium speed when the epithelial flap rises and from medium speed to top speed when the separator reaches the center of the cornea. Scanning electron microscopy of the stromal beds showed that the portions of the basement membrane were generally seen as island-like formations mainly in the center of the stromal bed, with the surrounding areas having mostly exposed regions of Bowman layer. These island-like formations were almost symmetrical to a straight line parallel to the hinge passing the center of the cornea. In addition, in the peripheral area of the stromal beds, the mostly exposed Bowman layer was seen in the region where the epithelial flap was cleaved initially as well as in the other peripheral regions. This result suggests that change of advance-head speed of the epikeratome we used may not affect separation layers.

Pallikaris et al.[12] assessed epithelial flaps after mechanical separation in epi-LASIK and found that the epithelial layers were separated beneath the basement membrane with intact epithelial basal cells, although they found that the basal epithelial cells rested on the prominent basal lamina with occasional focal disruptions. Katsanevaki et al.[24] also assessed inadvertently dislocated epithelial flaps and found that most epithelial cells were morphologically close to normal with minor cell degeneration. In a study by Kollias et al.,[21] the basal cell layer of the epithelial flap had normal morphology with interruptions of the basement membrane. However, Tanioka et al.[22] report that the basement membrane of the basal cells was partially or totally lost and the membrane of the basal cells was damaged in some regions. Microscopic and immunochemical evaluations in our study showed that epithelial separation occurred at 2 levels: within the lamina fibroreticularis with intact basal cells in some regions and along the lamina lucida with a damaged plasma membrane in other regions. Our results are similar to those reported by Tanioka et al.,[22] but not those of Pallikaris et al.[12] and Kollias et al.[21] Several possible reasons may account for this discrepancy and surgical devices can play a role. We used the same type epikeratome as Tanioka et al.; the type of epikeratome in the other 2 studies was a different model. Other factors, such as surgeon skill, surgical procedure, and corneal conditions, may affect the epithelial flap.

In conclusion, an epi-LASIK procedure using an Epi-K epikeratome mechanically separated the epithelial flap partially along the lamina lucida and within the lamina fibroreticularis in other regions. The device also provided a relatively smooth corneal surface with an intact Bowman layer and stroma after mechanical separation. Further studies are needed to determine which cleavage planes maintain cell viability of the epithelial flap and to enhance epithelial flap survival on the stromal bed postoperatively to reduce pain and haze after epi-LASIK.

REFERENCES

1. El-Maghraby A, Salah T, Waring GO III, Klyce S, Ibrahim O. Randomized bilateral comparison of excimer laser in situ keratomileusis and photorefractive keratectomy for 2.50 to 8.00 diopters of myopia. Ophthalmology 1999; 106:447–457
2. Hersh PS, Brint SF, Maloney RK, Durrie DS, Gordon M, Michelson MA, Thompson VM, Berkeley RB, Schein OD, Steinert RF. Photorefractive keratectomy versus laser in situ keratomileusis for moderate to high myopia; a randomized prospective study. Ophthalmology 1998; 105:1512–1522; discussion by JH Talamo, 1522–1523
3. Gimbel HV, van Westenbrugge JA, Anderson Penno EE, Ferensowicz M, Feinerman GA, Chen R. Simultaneous bilateral laser in situ keratomileusis; safety and efficacy. Ophthalmology 1999; 106:1461–1467; discussion by RK Maloney, 1467–1468
4. Stulting RD, Carr JD, Thompson KP, Waring GO III, Wiley WM, Walker JG. Complications of laser in situ keratomileusis for the correction of myopia. Ophthalmology 1999; 106:13–20
5. Tham VM-B, Maloney RK. Microkeratome complications of laser in situ keratomileusis. Ophthalmology 2000; 107:920–924
6. Autrata R, Rehurek J. Laser-assisted subepithelial keratectomy for myopia: two-year follow-up. J Cataract Refract Surg 2003; 29:661–668
7. Autrata R, Rehurek J. Laser-assisted subepithelial keratectomy and photorefractive keratectomy for the correction of hyperopia: results of a 2-year follow-up. J Cataract Refract Surg 2003; 29:2105–2114
8. Scerrati E. Laser in situ keratomileusis vs. laser epithelial keratomileusis (LASIK vs. LASEK). J Refract Surg 2001; 17: S219–S221
9. Chen CC, Chang J-H, Lee JB, Javier J, Azar DT. Human corneal epithelial cell viability and morphology after dilute alcohol exposure. Invest Ophthalmol Vis Sci 2002; 43:2593–2602. Available at: http://www.iovs.org/cgi/reprint/43/8/2593. Accessed March 11, 2009

10. Kim S-Y, Sah W-J, Lim Y-W, Hahn T-W. Twenty percent alcohol toxicity on rabbit corneal epithelial cells; electron microscopic study. Cornea 2002; 21:388–392
11. Pallikaris IG, Katsanevaki VJ, Kalyvianaki MI, Naoumidi II. Advances in subepithelial excimer refractive surgery techniques: epi-LASIK. Curr Opin Ophthalmol 2003; 14:207–212
12. Pallikaris IG, Naoumidi II, Kalyvianaki MI, Katsanevaki VJ. Epi-LASIK: comparative histological evaluation of mechanical and alcohol-assisted epithelial separation. J Cataract Refract Surg 2003; 29:1496–1501
13. Stepp MA, Spurr-Michaud S, Tisdale A, Elwell J, Gipson IL. α6β4 integrin heterodimer is a component of hemidesmosomes. Proc Natl Acad Sci USA 1990; 87:8970–8974. Available at: http://www.pubmedcentral.nih.gov/picrender.fcgi?artid=55082&blobtype=pdf. Accessed March 11, 2009
14. Tervo K, Tervo T, van Setten G-B, Virtanen I. Integrins in human corneal epithelium. Cornea 1991; 10:461–465
15. Adachi E, Hopkinson I, Hayashi T. Basement-membrane stromal relationships: interactions between collagen fibrils and the lamina densa. Int Rev Cytol 1997; 173:73–156
16. Zagon IS, Sassani JW, Ruth TB, McLaughlin PJ. Epithelial adhesion complexes and organ culture of the human cornea. Brain Res 2001; 900:205–213
17. Beuerman RW, Pedroza L. Ultrastructure of the human cornea. Microsc Res Tech 1996; 33:320–335
18. Pallikaris IG, Kalyvianaki MI, Katsanevaki VJ, Ginis HS. Epi-LASIK: preliminary clinical results of an alternative surface ablation procedure. J Cataract Refract Surg 2005; 31:879–885
19. Dai J, Chu R, Zhou X, Chen C, Qu X, Wang X. One-year outcomes of epi-LASIK for myopia. J Refract Surg 2006; 22:589–595
20. Katsanevaki VJ, Kalyvianaki MI, Kavroulaki DS, Pallikaris IG. One-year clinical results after epi-LASIK for myopia. Ophthalmology 2007; 114:1111–1117
21. Kollias A, Ulbig MW, Spitzlberger GM, Abdallat WH, Froehlich S, Welge-Luessen U, Lackerbauer C-A. Epi-LASIK using the Amadeus II microkeratome; evaluation of cut quality using light and electron microscopy. J Cataract Refract Surg 2007; 33: 2118–2121
22. Tanioka H, Hieda O, Kawasaki S, Nakai Y, Kinoshita S. Assessment of epithelial integrity and cell viability in epithelial flaps prepared with the epi-LASIK procedure. J Cataract Refract Surg 2007; 33:1195–1200
23. Weiss RA, Liaw L-HL, Berns M, Amoils SP. Scanning electron microscopy comparison of corneal epithelial removal techniques before photorefractive keratectomy. J Cataract Refract Surg 1999; 25:1093–1096
24. Katsanevaki VJ, Naoumidi II, Kalyvianaki MI, Pallikaris G. Epi-LASIK: histological findings of separated epithelial sheets 24 hours after treatment. J Refract Surg 2006; 22:151–154

First author:
Takeshi Soma, MD

Department of Ophthalmology, Osaka University Medical School, Osaka, Japan

Original article

A novel method of culturing human oral mucosal epithelial cell sheet using post-mitotic human dermal fibroblast feeder cells and modified keratinocyte culture medium for ocular surface reconstruction

Yoshinori Oie,[1,2] Ryuhei Hayashi,[1] Ryo Takagi,[3] Masayuki Yamato,[3] Hiroshi Takayanagi,[4] Yasuo Tano,[2] Kohji Nishida[1]

[1]Department of Ophthalmology and Visual Science, Tohoku University Graduate School of Medicine, Sendai, Japan
[2]Department of Ophthalmology, Osaka University Medical School, Suita, Japan
[3]Institute of Advanced Biomedical Engineering and Science, Tokyo Women's Medical University, Tokyo, Japan
[4]Translational Research Center, Tohoku University, Sendai, Japan

Correspondence to
Dr Kohji Nishida, Department of Ophthalmology and Visual Science, Tohoku University Graduate School of Medicine, Sendai 980-8574, Japan; knishida@oph.med.tohoku.ac.jp)

Accepted 20 February 2010

ABSTRACT

Background/aims To cultivate human oral mucosal epithelial cell sheets with post-mitotic human dermal fibroblast feeder cells and modified keratinocyte culture medium for ocular surface reconstruction.

Methods Human oral mucosal epithelial cells obtained from three healthy volunteers were cultured with x-ray-treated dermal fibroblasts (fibroblast group) and NIH/3T3 feeder layers (3T3 group) on temperature-responsive culture dishes. Media were supplemented using clinically approved products. Colony-forming efficiency was determined in both groups. Histological and immunohistochemical analyses were performed for cell sheets. Cell viability and purity of cell sheets were evaluated by flow cytometry.

Results Colony-forming efficiency in the fibroblast group was similar to that in the 3T3 group. All cell sheets were well stratified and harvested successfully. The expression patterns of keratin 1, 3/76, 4, 10, 12, 13, 15, ZO-1 and MUC16 were equivalent in both groups. The percentage of p63-positive cells in the fibroblast group (46.1±4.2%) was significantly higher than that in the 3T3 group (30.7±7.6%) ($p=0.038$, t test). The cell viability and purity were similar between the two groups.

Conclusion This novel culture method using dermal fibroblasts and pharmaceutical agents provides a safe cell processing system without xenogenic feeder cells for ocular surface reconstruction.

Tissue-engineered cell sheets composed of autologous oral mucosal epithelium have been successfully used to reconstruct eyes affected with severe ocular surface disorders.[1 2] However, it is possible that murine fibroblast feeder layers used for human transplantation can transmit murine diseases. In addition, it has been reported that human embryonic stem cells cultured on mouse feeder layers generate immunogenic non-human sialic acid.[3] Therefore, a new processing method that does not use animal-derived material should be developed to avoid this problem.

The use of human adipose tissue-derived and bone marrow-derived mesenchymal stem cells is reported to generate transplantable epithelial cell sheets.[4 5] The risks associated with xenogenic feeder layers can be avoided with these methods. However, the harvesting of adipose tissue or bone marrow is invasive; therefore, an alternative cell source for feeder layers is required for autologous cell therapy.

Dermal fibroblasts have been used as a feeder layer to culture skin keratinocytes,[6 7] and dermal fibroblast can be easily cultured.[8] It is thus thought that dermal fibroblasts can be utilised as an alternative candidate for mesenchymal stem cells or NIH/3T3 cells in culturing oral mucosal epithelial cells.

The supplements in conventional keratinocyte culture medium (KCM) are reagents used for laboratory research. The laboratory-grade supplements in KCM should be replaced with pharmaceutical products approved by the Ministry of Health, Labour and Welfare for clinical application. Modified KCM, which adopted the use of clinical agents as culture supplements, was equally as efficient as conventional KCM in the fabrication of canine, transplantable, stratified epithelial cell sheets.[9]

In particular, we investigated a novel culture method of human oral mucosal epithelial cell sheets using post-mitotic human dermal fibroblast feeder cells and modified KCM with clinically approved supplements.

MATERIALS AND METHODS

Preparation of feeder layers

Human dermal tissues were obtained from three healthy volunteers who provided written informed consent. Human tissue was handled according to the Declaration of Helsinki.

Dermal fibroblasts were cultured using the explant procedure.[8] To prepare feeder layers, human dermal fibroblasts were lethally irradiated with 40 Gly and then trypsinised and seeded onto tissue culture dishes (60 mm diameter; BD Biosciences, San Diego, California, USA) at a density of 5×10^3 cells/cm^2 (fibroblast group). As a positive control, lethally irradiated NIH/3T3 cells were prepared at a density of 2×10^4 cells/cm^2 (3T3 group).

Reverse transcription PCR

Total RNA was obtained from human dermal fibroblasts and NIH/3T3 cells using the GenElute mammalian total RNA kit (Sigma, St Louis, Missouri, USA). Reverse transcription was performed with the SuperScript First-Strand Synthesis System for reverse transcription PCR (Invitrogen, Carlsbad, California, USA), according to the manufacturer's suggested protocol, and cDNA was used as the template for PCR. The reverse transcription PCR thermocycle programme consisted of an initial step at 94°C for 5 min and 30 cycles at 94°C for 30 s and 58°C for 30 s and 72°C

for 30 s (PCR Thermal Cycler MP; Takara, Shiga, Japan). The primer pairs are shown in table 1.

Preparation of modified KCM

Modified KCM was supplemented with clinically approved products. The medium consisted of Dulbecco's modified eagle medium and Ham's F12 medium (Gibco-Invitrogen) at a 3:1 ratio, supplemented with 10% autologous human serum, 5 μg/ml insulin (humulin; Eli Lilly, Indianapolis, Indiana, USA), 2 nM triiodothyronine (thyronamin; Takeda, Osaka, Japan), 0.4 μg/ml hydrocortisone (saxizon; Kowa, Tokyo, Japan), 100 nM L-isoproterenol (proternol; Kowa), 2 mM L-glutamine (Gibco), 10 ng/ml epidermal growth factor (Higeta Shoyu, Chiba, Japan), and 40 μg/ml gentamicin (gentacin; Schering-Plough, Kenilworth, New Jersey, USA).

Oral mucosal epithelial cell culture

Human oral mucosal epithelial tissues were obtained from the same three healthy volunteers, respectively. Therefore, we performed the comparison of the two feeder layers three times in the current study. After the oral cavity of each volunteer was sterilised with topical povidone-iodine, a 3×3 mm specimen of oral mucosal tissue was surgically excised from the interior buccal mucosal epithelium under local anaesthesia with propitocaine. Oral mucosal epithelial cells were collected by removing all epithelial layers after treatment with dispase II (2.4 U/ml; Invitrogen), at 4°C for 4 h. Separated epithelial layers were treated with trypsin-EDTA (Invitrogen), and resuspended cells were plated on temperature-responsive culture inserts (CellSeed, Tokyo, Japan) at an initial cell density of 2.0×10^5 cells/23 mm insert, with feeder cells separated by cell culture inserts.[1] The cells were cultured for 14–17 days.

For colony-forming assays, 3000 or 5000 primary oral mucosal epithelial cells were seeded onto culture dishes (60 mm diameter; BD Biosciences) with irradiated feeder layers. After cultivation for 10–12 days, dishes were fixed and stained with rhodamine B. Colony-forming efficiency was defined as the ratio of the number of colonies to the number of cells inoculated. Colony size was also calculated using scanned photos of stained dishes with Axio Vision LE (Carl Zeiss, Jena, Germany).

Table 1 Primer sequences

Gene	Primer sequence (5′→3′)	Product size (bp)
hPTN	Forward: AGAGGACGTTTCCAACTCAA	551
	Reverse: TATGTTCCACAGGTGACATC	
hEPR	Forward: AGGAGGATGGAGATGCTCTG	498
	Reverse: TCAGACTTGCGGCAACTCTG	
hCC	Forward: TCCTCTCTATCTAGCTCCAG	500
	Reverse: TCCTGACAGGTGGATTTCGA	
hHGF	Forward: GCCTGAAAGATATCCCGACA	523
	Reverse: TTCCATGTTCTTGTCCCACA	
hKGF	Forward: AGGCTCAAGTTGCACCAGGCA	495
	Reverse: TGTGTGTCGCTCAGGGCTGGA	
hShh	Forward: CGGAGCGAGGAAGGGAAAG	262
	Reverse: TTGGGGATAAACTGCTTGTAGGC	
hIGF1a	Forward: ATGCACACCATGTCCTC	390
	Reverse: CATCCTGTAGTTCTTGTTTC	
hN-cad	Forward: ATGCTGACGATCCCAATG	317
	Reverse: GATGTCTACCCTGTTCTCA	
hGAPDH	Forward: ACCACAGTCCATGCCATCAC	452
	Reverse: TCCACCACCCTGTTGCTGTA	
mPTN	Forward: GGACCTCTGCAAGCCAAAAAA	317
	Reverse: GCACTCAGCTCCAAACTGCTTC	
mEPR	Forward: AGCTGCACCGAGAAAGAAGGA	318
	Reverse: AGAAGTGCTCACATCGCAGACC	
mCC	Forward: AGCTCGTGGCTGGAGTGAACTA	343
	Reverse: CCTGCAGCAGCTCCTTTACTGT	
mHGF	Forward: GGTGAAAGCTACAGAGGTCCCA	314
	Reverse: ATGGTATTGCTGGTTCCCCTG	
mKGF	Forward: CGAGGCAGACAGCAGACACGG	504
	Reverse: GTGTCGCTCGGGGCTGGAAC	
mShh	Forward: CCCAAAAAGCTGACCCCTTTAG	335
	Reverse: TCCACTGCTCGACCCTCATAGT	
mIGF1a	Forward: TATGGCTCCAGCATTCGGA	319
	Reverse: GCGGTGATGTGGCATTTTCT	
mN-cad	Forward: AGAGGGATCAAAGCCTGGGACGTAT	360
	Reverse: TCCACCCTGTTCTCAGGGACTTCTC	
mGADPH	Forward: ATCACTGCCACCCAGAAGACTG	325
	Reverse: TGCTGTTGAAGTCGCAGGAGA	

CC, cystatin C; EPR, epiregulin; GAPDH, glyceraldehydes-3-phosphate dehydrogenase; h, human; HGF, hepatocyte growth factor; IGF1a, insulin-like growth factor 1a; KGF, keratinocyte growth factor; m, mouse; N-cad, N-cadherin; PTN, pleiotrophin; Shh, sonic hedgehog.

Cell morphology

Cultured epithelial cells were observed under a phase contrast microscope, and microphotographs were taken at 100-fold magnification (Axiovert40; Carl Zeiss) to examine cell morphological aberrations and deficits.

Sheet recovery test

After examination with phase contrast microscopy, cultured epithelial cells were subjected to incubation at 20°C for 30 min. Then, a donut-shaped support membrane (18 mm outer diameter, 10 mm inner diameter, polyvinylidene difluoride; Millipore, Bedford, Massachusetts, USA) was placed on the epithelial cells. Finally, cells were challenged with harvesting in the presence of support membranes. Harvested epithelial cell sheets were divided into two parts. Half of the cell sheets were subjected to flow cytometry and the other half were subjected to histological analyses.

Cell viability and epithelial cell purity

Cell viability was evaluated with a dye exclusion test. An aliquot of cell suspension was incubated in Dulbecco's modified eagle medium with 7-aminoactinomycin D (BD Biosciences) staining at room temperature for 10 min, and subjected to flow cytometry (FACS Calibur; BD Biosciences).

After trypsin-EDTA treatment, an aliquot of the cell suspension was centrifuged, fixed and permeabilised with the Cytofix/Cytoperm kit (BD Biosciences) according to the manufacturer's protocol. Then, the cell suspension was split into two tubes, and incubated with either a FITC-conjugated anti-pancytokeratin IgG2a antibody (clone Pan1-8; Progen, Heidelberg, Germany) or a FITC-conjugated mouse control IgG2a antibody (Santa Cruz Biotechnology, Santa Cruz, California, USA) at room temperature for 60 min. After being washed twice with PBS, nuclei were stained with 7-aminoactinomycin D and the cells were examined by flow cytometry.

H&E staining and immunofluorescence analyses

The portion of cell sheets to be used in histological analyses was divided into two quadrants. One quadrant was fixed with formalin and embedded in paraffin. H&E staining was performed to observe the morphology and degree of stratification of the cultured epithelial cells. Microphotographs were taken with a light microscope (BZ-9000, Keyence, Osaka, Japan).

The other quadrant of cell sheets was embedded in Tissue-Tek OCT compound (Sakura Seiki, Tokyo, Japan) and processed into

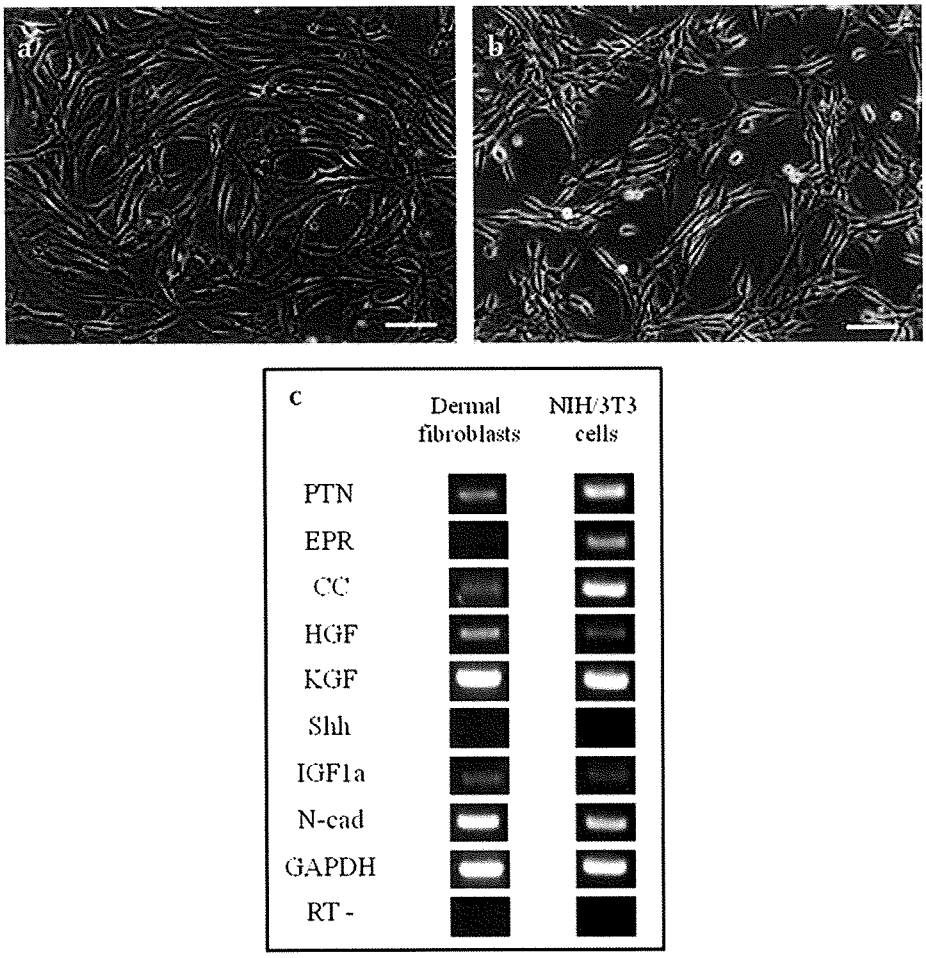

Figure 1 Feeder layers. Human dermal fibroblasts (a) and NIH/3T3 cells (b) were examined using phase-contrast microscopy. Gene expression was analysed by reverse transcription PCR. Both human dermal fibroblasts and NIH/3T3 cells expressed many factors for the maintenance of stem/progenitor cells and the growth of epithelial cells (c). Scale bars: 100 μm (a, b). CC, cystatin C; EPR, epiregulin; GAPDH, glyceraldehyde-3-phosphate dehydrogenase; HGF, hepatocyte growth factor; IGF1a, insulin-like growth factor 1a; KGF, keratinocyte growth factor; N-cad, N-cadherin; PTN, pleiotrophin; Shh, sonic hedgehog.

3-μm thick frozen sections. Cryosections from the cell sheets were immunostained with monoclonal antibodies against keratin 1 (K1, LHK1; Abcam, Cambridge, UK), keratin 3/76 (K3/76, AE5; Progen), keratin 4 (K4, 6B10; Abcam), keratin 10 (K10, DE-K10; DakoCytomation, Glostrup, Denmark), keratin 13 (K13, 1C7; American Research Products, Belmont, Massachusetts, USA), keratin 15 (K15, LHK15; Millipore), p63 (4A4; Santa Cruz Biotechnology), ZO-1 (1A12; Zymed, South San Francisco, California, USA), MUC16 (Ov185; Abcam), a polyclonal antibody against keratin 12 (K12, L-15; Santa Cruz Biotechnology), followed by incubation with Alexa488-labelled secondary antibodies (Molecular Probes, Eugene, Oregon, USA). Nuclei were co-stained with Hoechst 33342 (Sigma), and the cell sheets were mounted with PermaFluor (Beckman Coulter, Miami, Florida, USA). Slides were observed using confocal laser scanning microscopy (LSM-710; Carl Zeiss). The same concentration of corresponding normal, non-specific IgG was used as negative control. The percentage of p63 and K15-positive cells in each cultured cell sheet was calculated.

Statistical analysis

Data were analysed using t tests; $p<0.05$ was considered statistically significant.

RESULTS

Human dermal fibroblasts had morphological characteristics similar to those of NIH/3T3 cells (figure 1a,b). The gene expression pattern of dermal fibroblasts was similar to that of NIH/3T3 cells (figure 1c). Although dermal fibroblasts did not express epiregulin (EPR), other genes including pleiotrophin (PTN), cystatin C (CC), hepatocyte growth factor (HGF), keratinocyte growth factor (KGF), insulin-like growth factor 1a (IGF1a) and N-cadherin (N-cad) were expressed by both dermal fibroblasts and NIH/3T3 cells.

Colony-forming assays revealed that human dermal fibroblasts as well as NIH/3T3 cells are able to support the ex-vivo expansion of oral mucosal epithelial cells (figure 2a–d). The mean colony-forming efficiency of the primary cultures was 1.5±0.8% in the fibroblast group and 2.3±0.8% in the 3T3 group (mean±SD, n=3) (figure 2e), and the difference was not statistically significant ($p=0.266$, t test). The colony size in the fibroblast group (15.0±11.5 mm^2) was larger than that in the 3T3 group(6.4±2.1 mm^2). However, the difference was not statistically significant ($p=0.271$, t test).

Oral mucosal epithelial cell sheets were successfully cultured with human dermal fibroblasts and NIH/3T3 cells (figure 3a,b), and all of the cell sheets were successfully harvested by reducing the temperature to 20°C for 30 min. Therefore, all of the cell sheets passed the recovery test. The harvested cell sheets in both groups, flattened at their basal and apical surfaces, were composed of four to five layers of small basal cells, flattened middle cells and polygonal flattened superficial cells (figure 3c,d).

Immunofluorescence analyses revealed that cell sheets in both groups have a similar marker expression pattern (figure 4). K3/76, a marker for corneal and oral mucosal differentiated epithelial cells,[10] was positive in both groups. K12,

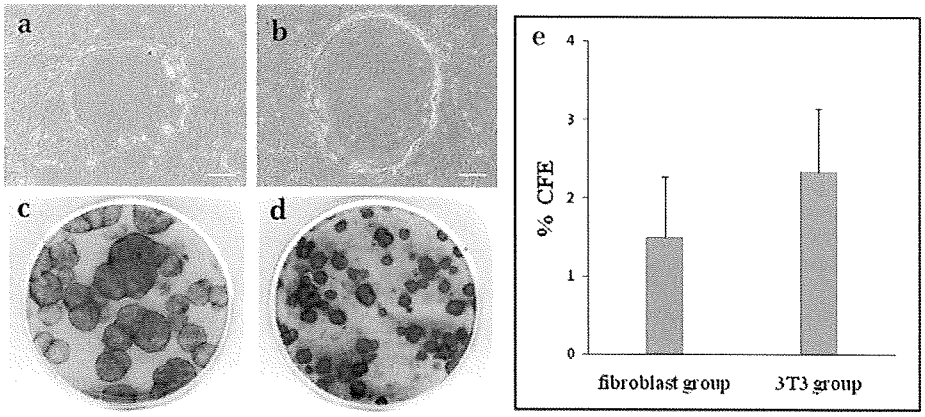

Figure 2 Colony-forming assay. Human dermal fibroblasts (a) as well as NIH/3T3 cells (b) supported the ex-vivo expansion of human oral mucosal epithelial cells. Cells were cultured for approximately 10 days, followed by fixation and staining with rhodamine B (c, dermal fibroblasts; d, NIH/3T3 cells). Colony-forming efficiency (CFE) was calculated, and no statistically significant differences were found between the human dermal fibroblasts and NIH/3T3 cells (e). Scale bars 100 μm (a, b).

a corneal-epithelium-specific marker,[10] was not expressed in either group. Although K4 and K13 are markers for mucosal stratified squamous epithelia,[11 12] only K4 was detected in the superficial cells in both groups. K1 and K10, markers for supra-basal cells in the epidermis,[13] were negative in both groups. ZO-1, a marker of tight junctions,[14] and MUC 16, a membrane associated-mucin specific to ocular surfaces, were expressed in both groups.

p63, which has been proposed to be a corneal epithelial stem/progenitor cell marker,[15] was expressed in the basal cells of both groups (figure 5a,b). The percentage of p63-positive cells in the fibroblast group (46.1±4.2%) was significantly higher than that in the 3T3 group (30.7±7.6%) (p=0.038, t test) (figure 5e). K15, a specific basal cell component of the epidermis and other stratified squamous epithelia,[16] was positive in basal cells in both groups (figure 5c,d). There were no significant differences between the percentages of K15-positive cells in the fibroblast group (24.0±3.7%) and the 3T3 group (20.6±2.5%) (p=0.257, t test) (figure 5f).

The cell viability of the cultured cell sheets in the fibroblast group and the 3T3 group was 88.7±4.1% and 85.9±3.5%, respectively. The purity of the epithelial cells in the cultured sheets was 98.2±1.9% and 96.3±3.6%, respectively. There were no statistical differences in cell viability (p=0.408, t test) or purity (p=0.466, t test) between the groups.

DISCUSSION

Dermal fibroblasts were shown to express many genes required for the maintenance of epithelial stem/progenitor cells and the proliferation of epithelial cells. Sugiyama *et al*[4] reported the expression of PTN, EPR, CC, HGF, KGF and IGF1a by human mesenchymal stem cells. In the current study, human dermal fibroblasts were confirmed to express N-cadherin in addition to these factors. The colony-forming efficiency with human dermal fibroblasts was similar to that with NIH/3T3 cells, and a colony-forming assay revealed that human dermal fibroblasts can expand oral mucosal epithelial cells well. In addition, immunofluorescence analyses revealed that cell sheets cultured with human dermal fibroblasts, as well as with NIH/3T3 cells, expressed markers such as K3/76, ZO-1, MUC16, p63, and K15. Moreover, cell sheets cultured with human dermal fibroblasts contained more p63-positive cells than those cultured with NIH/3T3 cells. Therefore, it was suggested that human dermal fibroblasts can maintain stem/progenitor cells in expansion more efficiently than NIH/3T3 cells.

The cultivation of epithelial cells with 3T3 feeder layers has been already established.[18] Also, a number of investigators has reported positive results for clinical treatments with cultured epithelial cells using 3T3 feeder layers.[1 18 19] However, 3T3 cells have the potential risk of transmitting murine infectious diseases. The use of xeno-free feeder cells, especially autologous

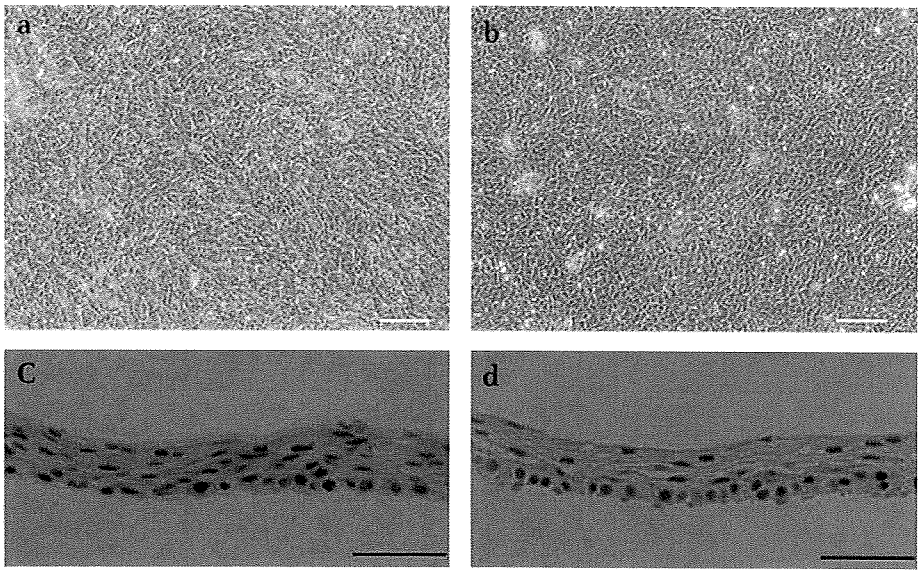

Figure 3 Human oral mucosal epithelial cell sheets. Examination of cell morphology was performed using phase-contrast microscopy (a, dermal fibroblasts; b, NIH/3T3 cells) and H&E staining (c, dermal fibroblasts; d, NIH/3T3 cells). Scale bars 100 μm (a, b), 50 μm (c, d).

Oie Y, Hayashi R, Takagi R, *et al*. *Br J Ophthalmol* (2010). doi:10.1136/bjo.2009.175042

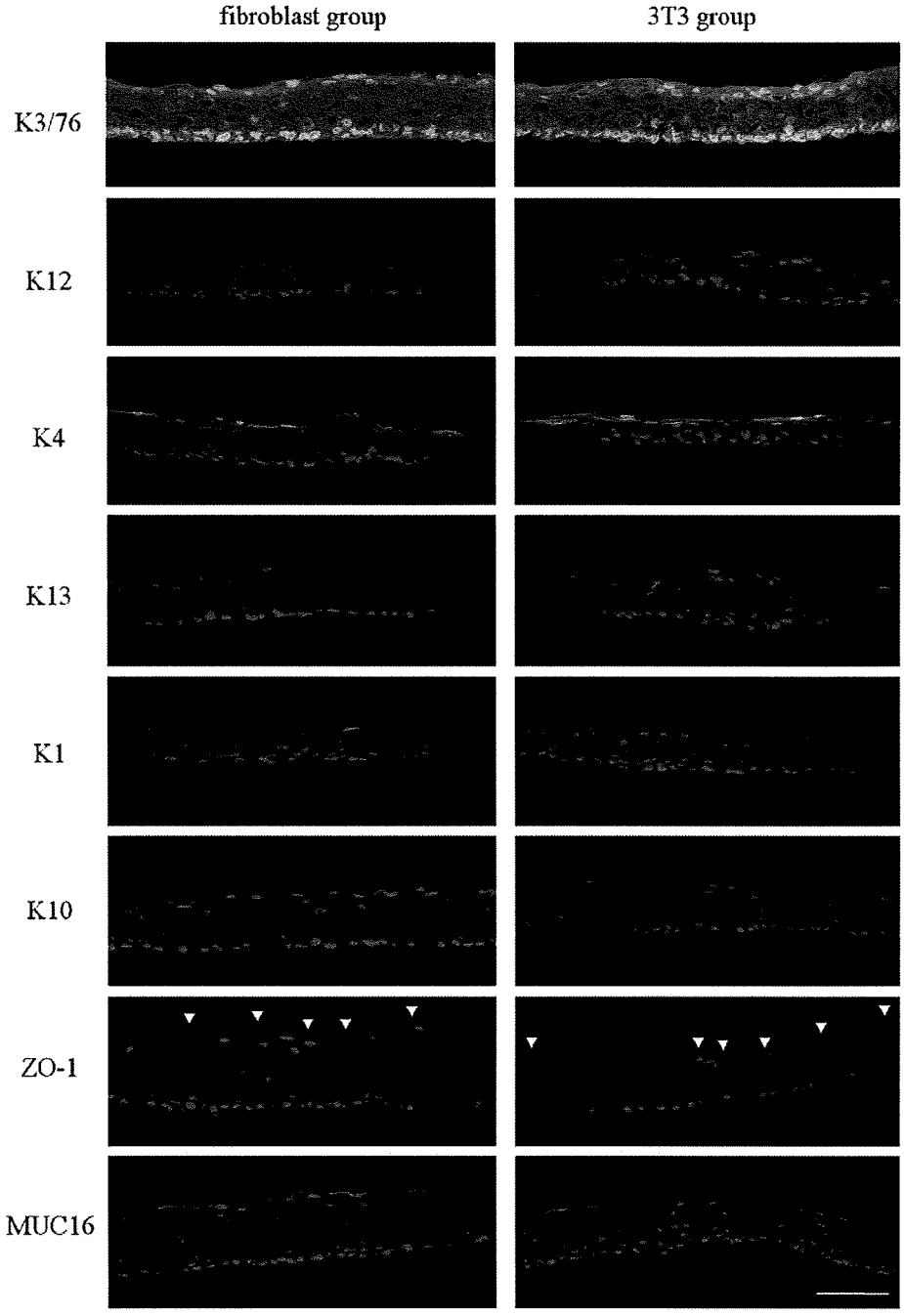

Figure 4 Immunohistochemical analyses of human oral mucosal epithelial cell sheets. Staining of human oral mucosal epithelial cell sheets cultured with dermal fibroblasts and NIH/3T3 cells with anti-keratin 3/76 (K3/76), anti-keratin 12 (K12), anti-keratin 4 (K4), anti-keratin 13 (K13), anti-keratin 1 (K1), anti-ZO-1 and anti-MUC16 antibodies. Nuclei were co-stained with Hoechst 33342. ZO-1 expression is marked with arrows. Scale bars 50 μm.

feeder layers, can prevent this problem. Although human adipose tissue-derived or bone marrow-derived mesenchymal stem cells can be used to generate transplantable epithelial cell sheets, dermal fibroblasts can be obtained with much less invasion to patients. Therefore, dermal fibroblasts are more desirable as an autologous feeder cell source than mesenchymal stem cells. Whereas the colony-forming efficiency of human limbal epithelial cells was 1.9±1.8% with bone marrow-derived mesenchymal stem cells,[5] that of human oral mucosal epithelial cells was 1.5±0.8% with human dermal fibroblasts in the current study. The colony-forming efficiency in these two reports cannot be compared directly, because of differences in the cultured epithelial cell type, media and sera. However, both feeder layers are thought to be able to generate transplantable epithelial cell sheets.

A xeno-free culture method of keratinocytes derived from skin using human dermal fibroblast has already been reported.[7] Therefore, it is well known that human dermal fibroblasts have a feeder effect on keratinocytes. Here, we cultured oral mucosal epithelial cells using human dermal fibroblast feeder layers. We are planning to use the cultured cell sheets for ocular reconstruction in future experiments. Zakaria *et al*[21] recently reported a new culture and transplantation method of limbal epithelial cells without xenogenic materials. If oral mucosal epithelial cells

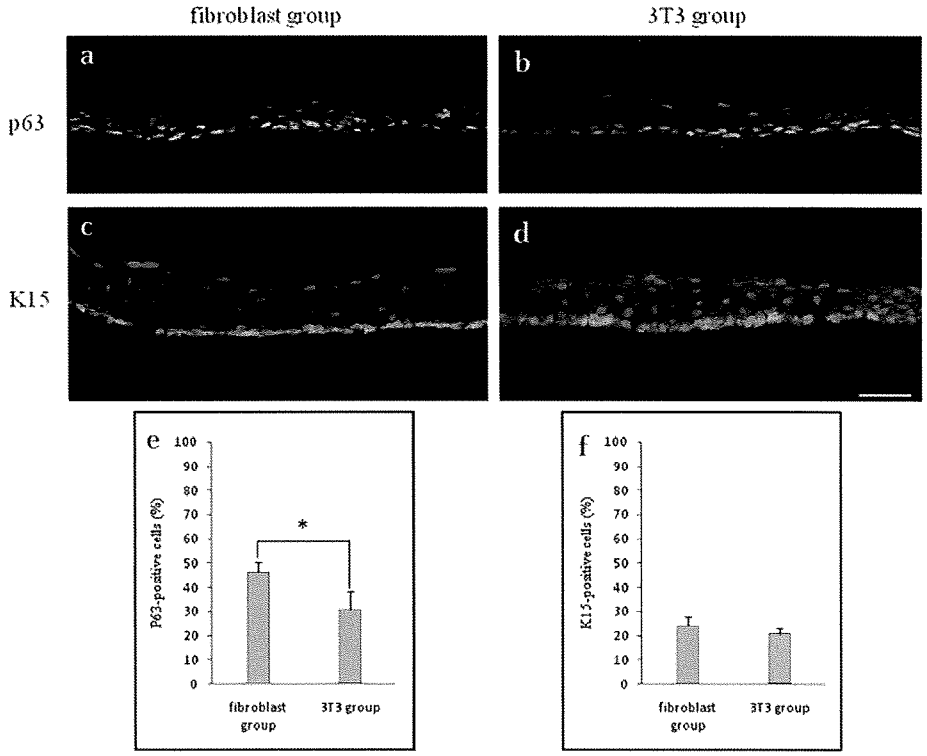

Figure 5 Analyses of human oral mucosal epithelial cell sheets for stem/progenitor markers. Anti-p63 staining (a, b) and anti-keratin 15 (K15) staining (c, d) of human oral mucosal epithelial cell sheets cultured with dermal fibroblasts and NIH/3T3 cells. Nuclei were co-stained with Hoechst 33342. Scale bar 50 μm. The percentage of p63-positive cells in the cell sheets cultured with dermal fibroblasts was significantly higher than that in cell sheets cultured with NIH/3T3 cells (e). The percentage of K15-positive cells was not significantly different between the groups (f). *$p<0.05$, t test.

can be cultured successfully, this method can also be an alternative to the method using 3T3 cells.

We recently developed a validation system for tissue-engineered epithelial cell sheets to be used in corneal regenerative medicine.[22] There has been no other established evaluation method for epithelial cell sheets before transplantation to date. However, the quality of cell sheets for clinical use can be standardised even in different facilities. We evaluated cell sheets using our validation method and obtained positive results. We thus believe that the oral mucosal epithelial cell sheets cultured with this method can be successfully used for ocular reconstruction.

It was previously reported that fibroblasts can affect the phenotypic characterisation of keratinocytes in co-culture.[22 23] However, epithelial cell sheets cultivated in the current study did not express K1 or K10, markers for suprabasal cells in the epidermis. Therefore, we propose that the phenotypic characterisation of keratinocytes cultured in the current study did not reflect that of the epidermis.

We also demonstrated that modified KCM worked well to generate oral mucosal epithelial cell sheets. Many methods using cholera toxin have been reported for the cultivation of human corneal or oral mucosal epithelial cells and human epidermal keratinocytes.[17 18 24] Agents known to increase the level of cellular cyclic AMP, including cholera toxin and isoproterenol, have been reported to increase the growth of colonies of cultured human epidermal cells and keratinocytes derived from other stratified squamous epithelia.[25] We also demonstrated the effectiveness of modified KCM with isoproterenol in the current study.

In conclusion, our novel culture system with post-mitotic human dermal fibroblast feeder cells with clinically approved products is effective and safe. Therefore, this system can be used as an alternative cultivation method for human oral mucosal epithelial cell sheets.

Funding This study was funded by the Ministry of Health Labor and Welfare, and the Ministry of Education, Culture, Sports, Science and Technology in Japan.

Competing interests None.

Ethics approval This study was conducted with the approval of the institutional review board of Tohoku University School of Medicine.

Provenance and peer review Not commissioned; externally peer reviewed.

REFERENCES

1. **Nishida K,** Yamato M, Hayashida Y, *et al.* Corneal reconstruction with tissue-engineered cell sheets composed of autologous oral mucosal epithelium. *N Engl J Med* 2004;**351**:1187–96.
2. **Nakamura T,** Inatomi T, Sotozono C, *et al.* Transplantation of cultivated autologous oral mucosal epithelial cells in patients with severe ocular surface disorders. *Br J Ophthalmol* 2004;**88**:1280–4.
3. **Martin MJ,** Muotri A, Gage F, *et al.* Human embryonic stem cells express an immunogenic nonhuman sialic acid. *Nat Med* 2005;**11**:228–32.
4. **Sugiyama H,** Maeda K, Yamato M, *et al.* Human adipose tissue-derived mesenchymal stem cells as a novel feeder layer for epithelial cells. *J Tissue Eng Regen Med* 2008;**2**:445–9.
5. **Omoto M,** Miyashita H, Shimmura S, *et al.* The use of human mesenchymal stem cell-derived feeder cells for the cultivation of transplantable epithelial sheets. *Invest Ophthalmol Vis Sci* 2009;**50**:2109–15.
6. **Bell E,** Ivarsson B, Merrill C. Production of a tissue-like structure by contraction of collagen lattices by human fibroblasts of different proliferative potential in vitro. *Proc Natl Acad Sci U S A* 1979;**76**:1274–8.
7. **Bullock AJ,** Higham MC, MacNeil S. Use of human fibroblasts in the development of a xenobiotic-free culture and delivery system for human keratinocytes. *Tissue Eng* 2006;**12**:245–55.
8. **Hayflick L,** Moorhead PS. The serial cultivation of human diploid cell strains. *Exp Cell Res* 1961;**25**:585–621.
9. **Takagi R,** Yamato M, Yang J, Preparation of keratinocyte culture medium for clinical applications for regenerative medicine. *J Tissue Eng Regen Med 2010*; In press. 4
10. **Schermer A,** Galvin S, Sun TT. Differentiation-related expression of a major 64K corneal keratin in vivo and in culture suggests limbal location of corneal epithelial stem cells. *J Cell Biol* 1986;**103**:49–62.
11. **Moll R,** Franke WW, Schiller DL, *et al.* The catalog of human cytokeratins: patterns of expression in normal epithelia, tumors and cultured cells. *Cell* 1982;**31**:11–24.
12. **Cooper D,** Schermer A, Sun TT. Classification of human epithelia and their neoplasms using monoclonal antibodies to keratins: strategies, applications, and limitations. *Lab Invest* 1985;**52**:243–56.
13. **Fuchs E,** Green H. Changes in keratin gene expression during terminal differentiation of the keratinocyte. *Cell* 1980;**19**:1033–42.

14. **Hayashida Y,** Nishida K, Yamato M, *et al*. Ocular surface reconstruction using autologous rabbit oral mucosal epithelial sheets fabricated ex vivo on a temperature-responsive culture surface. *Invest Ophthalmol Vis Sci* 2005;**46**:1632–9.
15. **Pellegrini G,** Dellambra E, Golisano O, *et al*. p63 identifies keratinocyte stem cells. *Proc Natl Acad Sci U S A* 2001;**98**:3156–61.
16. **Moll I,** Troyanovsky SM, Moll R. Special program of differentiation expressed in keratinocytes of human haarscheiben: an analysis of individual cytokeratin polypeptides. *J Invest Dermatol* 1993;**100**:69–76.
17. **Rheinwald JG,** Green H. Serial cultivation of strains of human epidermal keratinocytes: the formation of keratinizing colonies from single cells. *Cell* 1975;**6**:331–43.
18. **Pellegrini G,** Traverso CE, Franzi AT, *et al*. Long-term restoration of damaged corneal surfaces with autologous cultivated corneal epithelium. *Lancet* 1997;**349**:990–3.
19. **Nishida K,** Yamato M, Hayashida Y, *et al*. Functional bioengineered corneal epithelial sheet grafts from corneal stem cells expanded ex vivo on a temperature-responsive cell culture surface. *Transplantation* 2004;**77**:379–85.
20. **Kideryova L,** Lacina L, Dvorankova B, *et al*. Phenotypic characterization of human keratinocytes in coculture reveals differential effects of fibroblasts from benign fibrous histiocytoma (dermatofibroma) as compared to cells from its malignant form and to normal fibroblasts. *J Dermatol Sci* 2009;**55**:18–26.
21. **Zakaria N,** Koppen C, Van Tendeloo V, *et al*. Standardized limbal epithelial stem cell graft generation and transplantation. *Tissue Eng Part C Methods 2010*; In press. [5]
22. **Hayashi R,** Yamato M, Takayanagi H, *et al*. Validation system of tissue engineered epithelial cell sheets for corneal regenerative medicine. *Tissue Eng Part C Methods 2010*; In press. [6]
23. **Blazejewska EA,** Schlotzer-Schrehardt U, Zenkel M, *et al*. Corneal limbal microevironment can induce transdifferentiation of hair follicle stem cells into corneal epithelial-like cells. *Stem Cells* 2009;**27**:642–52.
24. **Yokoo S,** Yamagami S, Usui T, *et al*. Human corneal epithelial equivalents for ocular surface reconstruction in a complete serum-free culture system without unknown factors. *Invest Ophthalmol Vis Sci* 2008;**49**:2438–43.
25. **Green H.** Cyclic AMP in relation to proliferation of the epidermal cell: a new view. *Cell* 1978;**15**:801–11.

TISSUE ENGINEERING: Part C
Volume 00, Number 00, 2009

DOI: 10.1089/ten.tec.2009.0277

Methods Article

Validation System of Tissue-Engineered Epithelial Cell Sheets for Corneal Regenerative Medicine

Ryuhei Hayashi, Ph.D.,[1] Masayuki Yamato, Ph.D.,[2] Hiroshi Takayanagi, M.Sc.,[1] Yoshinori Oie, M.D.,[1] Akira Kubota, Ph.D., M.D.,[1] Yuichi Hori, Ph.D., M.D.,[3] Teruo Okano, Ph.D.,[2] and Kohji Nishida, M.D., Ph.D.[1]

Recently, regenerative therapy with tissue-engineered epithelial cell sheets has been performed for treating ocular surface disease. It would be required to develop the validation method for these cell sheets to standardize and spread the regenerative therapy. In the present study, we developed a validation system for cultivated epithelial cell sheets. Human limbal epithelial cells and human oral mucosal epithelial cells were cultured with 3T3 feeder layer cells on temperature-responsive culture inserts for three different culture periods, and subjected to cell sheet harvest and validation. Epithelial cells cultured for a short period were not successfully harvested as intact contiguous cell sheets. On the other hand, total cell number and viability of epithelial cell sheets harvested after prolonged culture period decreased. Further, these cells also lost epithelial barrier function. These results showed the potential effectiveness of the proposed validation system that can evaluate fabricated cell sheets before transplantation.

Introduction

Corneal epithelial stem cells reside in the basal layer of the limbus, the transitional zone between the cornea and the bulbar conjunctiva.[1] These cells govern renewal of the corneal epithelium by generating progeny (transient amplifying cells, which are the cells committed to epithelial differentiation) with limited renewal capabilities that migrate from the limbus into the basal layer of the cornea.[2,3] If corneal epithelial stem cells are completely absent owing to limbal disorder from severe trauma or eye diseases, then the sources of corneal epithelial cells have been exhausted, the peripheral conjunctival epithelium invades inwardly, and the corneal surface becomes enveloped by vascularized conjunctival scar tissue, resulting in corneal opacification that leads to severe visual impairment. Such pathological characteristics are considered to represent limbal stem-cell deficiencies.[4,5]

For patients with unilateral or bilateral limbal stem-cell deficiencies, limbal allograft transplantation can be performed,[6] but it requires long-term immunosuppression that involves high risks of serious eye and systemic complications, including infection and liver and kidney dysfunction.[7] In patients with the Stevens–Johnson syndrome or ocular pemphigoid, graft failure is common, even with immunosuppression, owing to serious preoperative conditions such as persistent inflammation of the ocular surface, abnormal epithelial differentiation of the ocular surface, severe dry eyes, and lid-related abnormalities.[7–9] Therefore, we have performed a regenerative therapy for such patients with severe corneal epithelial disease by transplantation of functional tissue-engineered epithelial cell sheets fabricated on temperature-responsive culture surfaces.[10,11] By utilizing temperature-responsive culture surfaces, noninvasive cell sheet harvest is reproducibly achieved, since the surfaces reversibly change the hydrophobic/hydrophilic property depending on temperature across 32°C. Only by reducing temperature below 32°C, all the cultured cells are harvested as a single contiguous cell sheet without need for proteolytic enzymes. Cell sources are patient's own healthy limbus and oral mucosa for unilateral and bilateral disease cases, respectively.

Recently, several groups have also reported similar epithelial cell transplantation to treat ocular surface disease.[12–14] These reports, including ours, showed that epithelial cell sheet transplantation was effective in the treatment of severe ocular surface diseases. However, there are no detailed descriptions regarding the cell sheet quality that would be assessed by each researcher. Moreover, it is now the next step to develop the corneal epithelial regenerative therapy from clinical trials into a standard medical therapy, and for this it is important to precisely validate the final products before transplantation to determine whether they can be used or not. Here we would like to propose a validation system

[1]Department of Ophthalmology, Tohoku University Graduate School of Medicine, Sendai, Japan.
[2]Institute of Advanced Biomedical Engineering and Science, Tokyo Women's Medical University, Tokyo, Japan.
[3]Department of Ophthalmology, Osaka University School of Medicine, Suita, Japan.

composed of the following evaluation items: (1) cell morphology, (2) cell sheet recovery, (3) total cell number, (4) cell viability, (5) epithelial cell purity, (6) degree of stratification, (7) existence of epithelial stem/progenitor cells, (8) cell differentiation, and (9) existence of barrier function. In the present study, we evaluated transplantable human epithelial cell sheets with different culture periods to confirm the usefulness of the proposed validation system.

Materials and Methods

Epithelial cell culture

Human limbal tissues were isolated from corneoscleral rims isolated from cadaveric donor corneas (Northwest Lions Eye Bank, Seattle, WA) using scissors ($n = 4$). Human oral mucosal tissue ($\sim 3 \times 3$ mm specimen) was surgically excised from a healthy volunteer's interior buccal mucosa under local anesthesia with xylocaine ($n = 3$). Each tissue was washed with Dulbecco's phosphate-buffered saline containing antibiotics and antimycotics, and incubated with dispase II at 37°C for 1 h. Separated epithelial layer was treated with trypsin–ethylenediaminetetraacetic acid (EDTA) solution (Invitrogen, Carlsbad, NM), and resuspended cells were plated on temperature-responsive culture inserts (CellSeed, Tokyo, Japan) at an initial cell density of 1.5×10^5 cells (limbal epithelial cells) or 2.0×10^5 cells (oral mucosal epithelial cells)/23-mm insert with mitomycin C–treated NIH/3T3 cells separated by cell culture inserts in the keratinocyte culture medium (KCM) (Dulbecco's modified Eagle's medium [DMEM]/F12 [3:1] supplemented with 10% fetal bovine serum [Japan Bio Serum, Hiroshima, Japan], 0.5% Insulin–Transferrin–Selenium [ITS; Invitrogen], 10 μM isoproterenol [Kowa, Tokyo, Japan], 2.0×10^{-9} M triiodothyronine [MP Biomedicals, Aurora, OH], 0.4 μg/mL hydrocortisone succinate [Wako, Osaka, Japan], and 10 ng/mL EGF [R&D Systems, Minneapolis, MN]).[10] All the procedures for the validation system were performed within the day when the cell culture was terminated (Fig. 1).

Phase contrast microscopy

The cultured epithelial cells were observed under a phase contrast microscope, and microphotographs were taken at 50-fold and 100-fold magnification (Axiovert 40; Carl Zeiss, Jena, Germany) to examine cell morphological aberration and deficits.

Sheet recovery test

After being examined by phase contrast microscopy, the cultured epithelial cells were subjected to incubation at 20°C for 30 min in an incubator of 5% CO_2. Then, a donut-shaped support membrane (18 mm in outer diameter and 10 mm in inner diameter; polyvinylidene difluoride; Millipore, Bedford, MA) was placed on the epithelial cells. Finally, the cells were challenged to cell sheet harvest together with support membranes. The harvested epithelial cell sheets were bisected. One of the bisected cell sheets was subjected to counting of total cell number and flow cytometric analyses, and the other was subjected to histological analyses (Fig. 1).

Total cell number

Bisected cell sheets were incubated with 0.25% trypsin–EDTA at 37°C for 10 min to obtain single-cell suspension. The enzymatic reaction was stopped by adding DMEM containing 5% fetal bovine serum. After centrifugation, the cells were resuspended in DMEM, and the cell number was counted with a Burker–Turk hemocytometer.

Cell viability

Cell viability was evaluated with dye exclusion test. An aliquot of cell suspension was incubated in DMEM with 7-aminoactinomycin D (7′AAD; BD Biosciences, San Diego, CA) staining at room temperature for 10 min, and subjected to flow cytometer (FACS Calibur; BD Biosciences).

Epithelial cell purity

An aliquot of cell suspension after trypsin–EDTA treatment was centrifuged, fixed, and permeabilized with Cytofix/Cytoperm kit (BD Biosciences) according to the manufacturer's protocols. Then, the cell suspension was split into two tubes, and reacted with either fluorescein isothiocyanate–conjugated antipancytokeratin immunoglobulin G2a (IgG2a) antibody (clone PAn1-8; Progen, Heidelberg, Germany) or fluorescein isothiocyanate–conjugated mouse control IgG2a antibody (Santa Cruz Biotechnology, Santa Cruz, CA) at room temperature for 60 min. After being washed with phosphate-buffered saline twice, the cells were stained with 7′AAD for the nuclear staining and examined by flow cytometry.

Hematoxylin and eosin staining

Hematoxylin and eosin (HE) staining was performed on the other bisected cell sheets to examine the degree of stratification of epithelial cells in the harvested cell sheets. The bisected cultured epithelial cell sheets were embedded in Tissue-Tek® O.C.T™ compound (Sakura Seiki, Tokyo, Japan), and processed into 10-μm-thick frozen sections. After being dried for 1 h at room temperature, tissues were washed three times with Tris-buffered saline (TBS; Takara Bio, Shiga, Japan), and fixed with 10% formaldehyde at room temperature for 30 min. The sections were washed with TBS twice and then stained with HE. Microphotographs were taken with a light microscope (Carl Zeiss, Jena, Germany), and the degree of stratification was examined.

Immunofluorescence analyses

Frozen sections were incubated with TBS containing 5% donkey serum and 0.3% Triton X-100 for 1 h to block nonspecific reactions. Sections were then incubated with anti-p63 antibody (4A4; Santa Cruz Biotechnology), anti-cytokeratin 3/2p antibody (AE5; Progen), anti-ZO-1 antibody (1A12; Zymed, South San Francisco, CA), or anti-MUC16 antibody (Ov185; AbCam, Cambridge, United Kingdom) at room temperature for 1.5 h. The slides were washed with TBS twice and then incubated with Alexa Flour 488–conjugated anti-mouse IgG antibody (Molecular Probes, Eugene, OR) at room temperature for 1 h. After being washed with TBS twice, the sections were counterstained with Hoechst 33342 (Molecular Probes) for 10 min and mounted with Perma-Fluor (Beckman Coulter, Miami, FL). The slides were observed using fluorescent microscopy (Axiovert 40; Carl Zeiss).

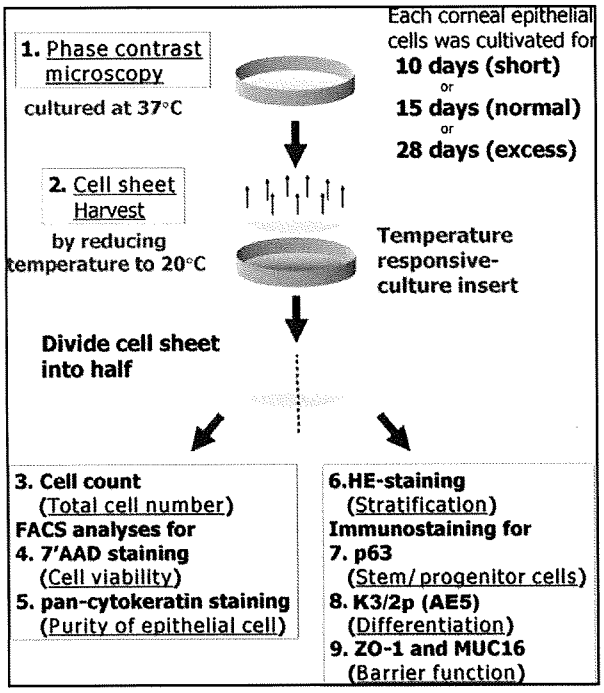

FIG. 1. Validation system. Human limbal epithelial cells were cultured on temperature-responsive cell inserts for 10, 15, and 28 days. Cell morphological examination was performed by phase contrast microscopy, and then cultured epithelial cells were harvested by reducing temperature to 20°C. Harvested cell sheets were divided into two halves. One was used for cell counting and flow cytometric analyses, and the other for hematoxylin and eosin (HE) staining and immunostaining for p63, K3/2p, ZO-1, and MUC16, to validate the quality of cell sheets. All of these procedures were performed within the day when cell culture was terminated.

Results

Phase contrast microscopy revealed that human epithelial cells obtained from a piece of limbal tissue proliferated and stratified on day 15 under the present culture condition. These cells showed tight and dense packing on culture inserts as well as cobble stone–like cell morphology, which is specific to stratified squamous epithelial cells (Fig. 2). In contrast, cell density was still low on day 10. Some defects and denucleated cells were found on day 28. Coinciding with the phase contrast microscopic results, all the epithelial cells on the temperature-responsive culture insert were successfully harvested as a single contiguous cell sheet on day 15. No defects or damage was observed in the harvested cell sheets. Similarly, all the epithelial cell sheets cultured for 28 days were also harvested as cell sheets, but the harvested cell sheets were more fragile than those cultured for 15 days and partially broken. These epithelial cells cultured for 10 days were not harvested as cell sheets, implying insufficient cell packing and stratification. Averages of total cell number in corneal epithelial cell sheets harvested on days 15 and 28 were 11.0×10^5 and 5.1×10^5 cells, respectively. Dye exclusion tests with flow cytometric analysis after membrane-impermeable 7'AAD staining revealed that cell viability was satisfying on day 15 (93.2%), but significantly decreased (64.1%) after prolonged culture of 28 days (Fig. 3). However, epithelial cell purity of the harvested cell sheets determined by flow cytometric analysis after pancytokeratin staining was essentially the same in both of the cell sheets (>95%) (Fig. 3).

Stratification of epithelial cells in harvested sheets was evaluated on HE-stained sections (Fig. 4). Epithelial cell sheets harvested on day 15 comprised of four to eight layers of epithelial cells, and each stratified layer resembled basal, wing, and superficial squamous epithelial cells in morphology as observed in native corneal epithelia. However, fragile cell sheets harvested on day 28 comprised of only one to three epithelial cell layers. p63, a marker of epithelial stem/progenitor cells,[15,16] was expressed in the basal cell layers of both the harvested cell sheets (Fig. 4). Cells positively reacted with anti-cytokeratin 3/2p (corneal and oral mucosal differentiated epithelial cell markers)[1] monoclonal antibody (clone AE5) detected predominantly in both cell sheets, but it was faint in the basal cell layer of cell sheets harvested on day 15. Two essential molecules for epithelial barrier function of ZO-1 in tight junctions[17] as well as a membrane-associated mucin, MUC16, specific to ocular surfaces[18] were expressed continuously throughout superficial cells in cell sheets harvested on day 15. On the other hand, ZO-1 and MUC16 were faintly and discontinuously expressed in the superficial cells in cell sheets harvested on day 28. These results are summarized in Table 1.

In our protocol for corneal regenerative therapy, patients' own oral mucosal tissues are used as an epithelial cell source in bilateral cases.[19,20] Therefore, we performed the present validation for not only human corneal epithelial cell sheets (Fig. 5; $n=3$), but also human oral mucosal epithelial cell sheets ($n=3$) cultured for appropriate periods of 13–16 days determined by the phase contrast microscopic observation. The result showed that there were no remarkable differences between oral mucosal and corneal epithelial cell sheets in each examination (Table 2). Each examination was performed stably in every cell sheet validation.

Discussion

In this study, we performed the validation of the epithelial cell sheet based on the following evaluation items: (1) cell morphology, (2) cell sheet recovery, (3) total cell number, (4) cell viability, (5) epithelial cell purity, (6) degree of stratification, (7) existence of epithelial stem/progenitor cells, (8) differentiation state, and (9) existence of barrier function. Obtained results show that this validation system successfully detected differences in the quality of corneal epithelial cells cultured for different periods. With the same methods, we reproducibly performed the validations of human corneal and oral mucosal epithelial cell sheets cultured for appropriate periods.

In this validation system, cell sheet recovery test could be the most important, because cell sheets are fabricated on temperature-responsive culture surfaces and have no carriers for transplantation such as amniotic membrane or type I collagen sheets. In the present study, it was shown that cell sheets were too fragile for harvest and transplantation after 10-day culture. This might be caused by insufficiency of cell number, cell stratification, intercellular adhesion, and deposition of extracellular matrix. This finding also indicated that